

1 Generating nanoliter to femtoliter microdroplets with ease

AQ:
#1

2 R. Grossier,^{1,a)} Z. Hammadi,¹ R. Morin,¹ A. Magnaldo,² and S. Veessler^{1,a)}
 3 ¹Centre Interdisciplinaire de Nanoscience de Marseille (CINAM), CNRS, Aix-Marseille University,
 4 Campus de Luminy, Case 913, 13288 Marseille Cedex 09, France
 5 ²DRCP/SE2A/LEHA, CEA-Valrhô, BP17171, 30207 Bagnols-sur-Cèze, France

6 (Received 10 November 2010; accepted 6 February 2011; published online xx xx xxxx)

7 In this letter, we present a simply constructed and easy-to-use fluidic device that generates arrayed
 8 aqueous phase microdroplets in oil of controlled size with volumes ranging from nanoliter to
 9 femtoliter without surfactant. This can be applicable with a range of materials, allowing production
 10 and storage of monodisperse microdroplets. We illustrate the potential of our methodology in the
 11 field of nanoparticle generation © 2011 American Institute of Physics. [doi:10.1063/1.3560453]
 12

13 Producing microdroplets,¹ droplets in the micrometer
 14 range, is of interest in many fields, including biology, bio-
 15 medical applications, drug discovery, chemical synthesis,
 16 and particle synthesis (for photonics materials, drug deliv-
 17 ery). In the literature, different approaches to microdroplet
 18 generation are presented, from the classical emulsion-based
 19 method or bulk method² to the more recent droplet
 20 microfluidics.³ To date, a significant problem encountered
 21 when forming droplets via bulk methods, the top-down ap-
 22 proach, is the wide microdroplet size distribution that typi-
 23 cally results.⁴ This is remedied by emulsification at the indi-
 24 vidual droplet level, the bottom-up approach, based on the
 25 ability of microfluidics devices to generate, control, and
 26 handle microdroplets. One of the limitations of these ap-
 27 proaches is that necessitate the use of surfactant to achieve
 28 well-defined structures (droplets) and to avoid droplet coa-
 29 lescence during storage. These surfactants affect chemical
 30 composition and fluid interface properties. Another limitation
 31 of microfluidics is that it is impossible to produce an ordered
 32 pattern for channel sizes below 100 nm, because of wetting
 33 properties.⁵ Conversely, the classical emulsion-based method
 34 can generate droplets in the nanometer range.⁶ Microfluidics
 35 experiments are often referred to as “high-throughput droplet
 36 generation.”¹ However, lower-throughput experiments, from
 37 generation of a single droplet to dozens of droplets, using
 38 nozzles or pipette have also been developed: for instance,
 39 levitation of a single droplet,⁷ isolated droplets held by a
 40 micropipette⁸ or nanoscale pipetting.⁹ Note that some authors
 41 describe a nozzle-free acoustic ejector^{10,11} which has limita-
 42 tions due to possible liquid evaporation. All these technolo-
 43 gies are efficient but require a complex setup.

44 In this letter, we present a simply constructed and easy-
 45 to-use fluidic device that generates arrayed aqueous phase
 46 microdroplets in oil. Up to thousands of microdroplets are
 47 generated with volumes ranging from nanoliter to femtoli-
 48 ters, without surfactant. The device enables the entire volume
 49 range to be attained in the course of one experiment. All
 50 experiments are performed on an 18 mm diameter coverslip
 51 treated in a way to obtain an hydrophobic surface to avoid
 52 microdroplet spreading and coalescence, which can be ther-
 53 mostatted, under an optical microscope (Zeiss Axio Observer
 54 D1). Glass coverslip are spin coated at 4000 rpm for 1 min

(SPIN 150, SPS) with 4%-950 K PMMA (All Resist ARP 55
 679.04) annealed 10 min at 170 °C. The coverslip is covered 56
 with approximately 100 μl of paraffin oil (Hampton Re- 57
 search HR3-421, refractive index=1.467). The micrometer 58
 sized droplets of water solution are generated on the cover- 59
 slip by a microinjector (Femtojet, Eppendorf) used for the 60
 injection of liquids in the volume range from femtoliters to 61
 microliters. A home-made micromanipulator consisting of 3 62
 miniature translation stages (piezo electric, MS30 Mechon- 63
 ics) allows displacement of the injector (capillary holder) in 64
 X, Y, and Z with a displacement of 18 mm in the three 65
 directions by steps of 16 nm. A glass capillary (the micropi- 66
 pette) with an internal diameter of 0.5 μm (Femtotip Eppen- 67
 dorf) is used. The whole setup is shown in Fig. 1. Here the 68
 solution is 2.71 M NaCl aqueous solution, half the solubility 69
 of NaCl in water at 20 °C.¹² Our first experiments with dif- 70
 ferent solution compositions show the importance of interfa- 71
 cial tension between phases and viscosities of phases for the 72
 control of the microdroplet sizes; however, the mechanism of 73
 microdroplet generation is independent of the solution com- 74
 position, as pointed out by Tabeling *et al.*¹³ in the case of 75
 microfluidics. Note that, here, we succeeded in generating 76
 microdroplets with many aqueous phases tested.¹⁴ By con- 77
 trolling the speed displacement of the micropipette (in con- 78
 tact with the surface) and injection pressure we control the 79
 droplet size. In Fig. 2(a) we show an array of monodisperse¹⁵ 80
 water droplets of mean size $11.8 \mu\text{m} \pm 0.6 \mu\text{m}$. When the 81
 speed displacement of the micropipette is varied from 1 to 82
 0.1 mm s^{-1} , the droplet size varies from 12 to 31 μm [Fig. 83

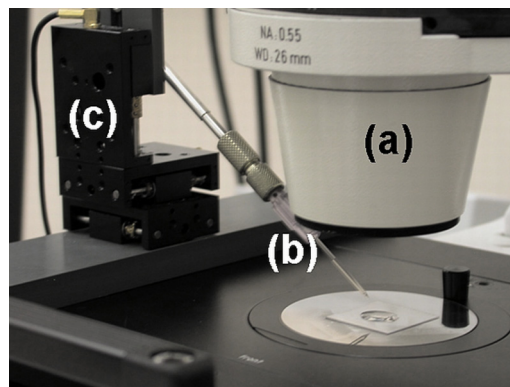
AQ:
#2

FIG. 1. (Color online) Image of the whole experimental setup, (a) microscope, (b) glass capillary, and (c) XYZ miniature translation stages.

^{a)}Authors to whom correspondence should be addressed. Electronic addresses: grossier@cinam.univ-mrs.fr and veessler@cinam.univ-mrs.fr.

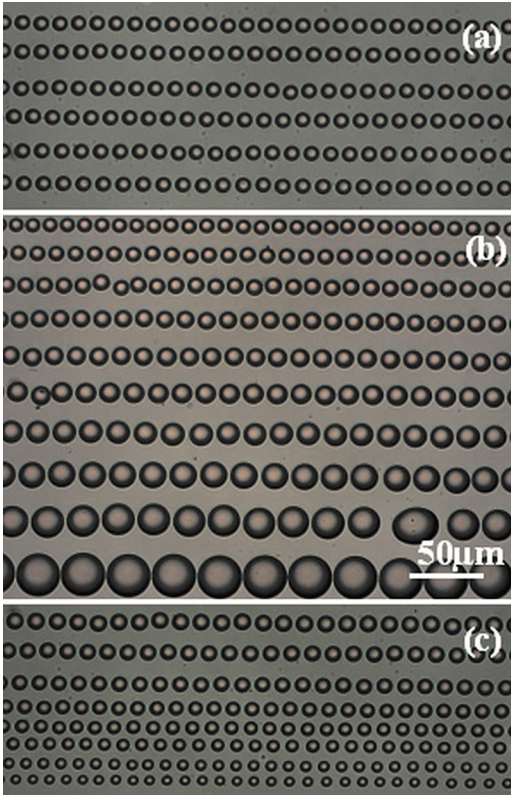


FIG. 2. (Color online) (a) Image of droplets generated with $P=5000$ Pa and $v=1$ mm s⁻¹, (b) Image of droplets generated with $P=4000$ Pa and v varying from 0.1 (first line) to 1 mm s⁻¹ (last line) by 0.1 mm s⁻¹ step, and (c) Image of droplets generated with $v=1$ mm s⁻¹ and P varying from 5000 Pa (first line) to 1500 Pa (last line) by 500 Pa step. All images are at the same magnification: 1 pixel=0.5625 μm. (enhanced online) [URL: <http://dx.doi.org/10.1063/1.3560453.1>]

84 2(b), see video]. Furthermore, when the injection pressure is
85 varied from 1500 to 6000 Pa, the droplet size varies from 8.5
86 to 14 μm [Fig. 2(c)]. Mean diameter variations as a function
87 of distance between droplets, speed displacement, and injec-
88 tion pressure are plotted in Fig. 3.

89 We analyze the micropipette velocity v influences on
90 experimental results in the frame of a simple model. The
91 distance d between droplets is as follows:

$$92 \quad d = v \times t, \quad (1)$$

93 where t the time interval between successive droplet forma-
94 tions. The volume V of the droplet is as follows:

$$95 \quad V = \eta \times t, \quad (2)$$

96 where η is the flow rate from the micropipette. From Eqs. (1)
97 and (2) we deduce that

$$98 \quad V = \frac{\eta \times d}{v}. \quad (3)$$

99 Assuming a spherical shape for the droplet with a diameter
100 D , thus

$$101 \quad V = \frac{\pi}{6} \times D^3 \quad (4)$$

102 leads to the following:

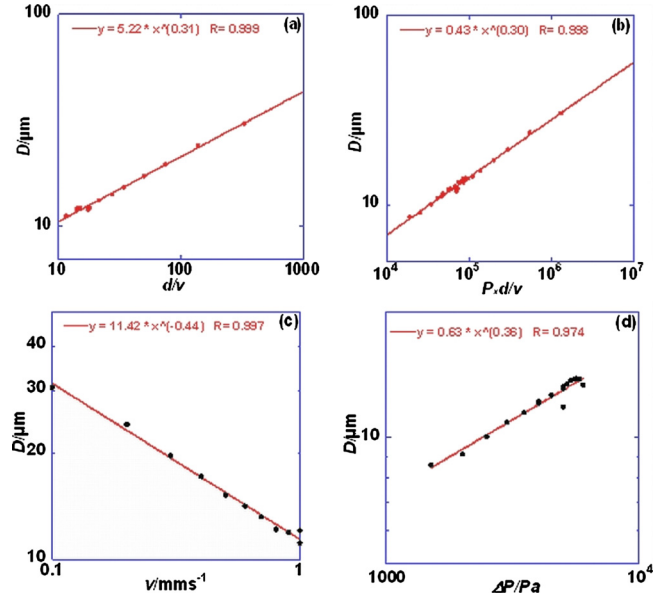


FIG. 3. (Color online) Droplet diameter vs (a) distance between droplets over speed displacements at $\Delta P=4000$ Pa, (b) distance between droplets with ΔP varying between 1500 and 6000 Pa, (a) and (b) v varying between 0.1 and 1 mm s⁻¹, (c) speed displacements at injection pressure of 5000 Pa and, (d) injection pressures at speed displacement of 1 mm s⁻¹.

$$D = \left(\frac{6 \times \eta}{\pi} \right)^{1/3} \times \left(\frac{d}{v} \right)^{1/3} \quad (5a) \quad 103$$

in a first approximation, ignoring dynamic factors, we as- 104
sume proportionality between flow rate and injection pres- 105
sure ΔP 106

$$D = A \times \left(\frac{\Delta P \times d}{v} \right)^{1/3}, \quad (5b) \quad 107$$

where A is a constant. Figure 3(a), a plot of D vs d/v at 108
 $\Delta P=4000$ Pa, gives $D \propto (d/v)^{0.31}$ and Fig. 3(b), a plot of D 109
vs $\Delta P \times d/v$, gives $D \propto (\Delta P \times d/v)^{0.30}$ showing a very good 110
experimental agreement with Eqs. (5a) and (5b). 111

We take the analysis further by introducing the mecha- 112
nism of drop formation through the Rayleigh–Plateau insta- 113
bility as follows:¹⁶ the flow generated by the microinjector 114
passes through the exit orifice and breaks up to form drops, 115
assuming a cylindrical stream (a liquid jet breaks because the 116
surface energy of a liquid sphere is smaller than that of a 117
cylinder, while having the same volume). If we assume that 118
the fluid flowing out of the micropipette is a cylinder of 119
radius r and length d (d is also the distance between drop- 120
lets), the instability occurs for the following: 121

$$\frac{r}{d} = B, \quad (6) \quad 122$$

where B is a constant (critical ratio in the Raleigh–Plateau 123
instability). V the volume of fluid flowing out of the pipette 124
during time t [Eq. (2)], is equal to the volume of the cylinder 125
at t , thus 126

$$V = \eta \times t = v \times t \times \pi \times r^2. \quad (7) \quad 127$$

Combining Eqs. (6), (7), and (1) gives the following: 128

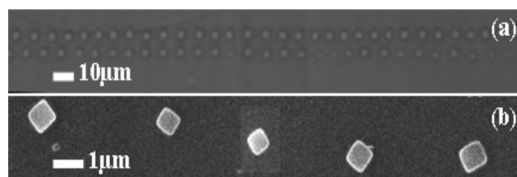


FIG. 4. (a) Array of droplets of NaCl solutions generated through the layer of liquid oil. The size of droplets is 3 μm corresponding to an effective volume of 14 fl, and (b) SEM images of single crystals generated.

$$D = (6 \times B^2)^{1/3} \times d \quad (8)$$

showing the linear dependence of D with d . Combining Eqs. (6) and (7) gives the following:

$$d = \frac{1}{B} \sqrt{\frac{\eta}{\pi \times v}} = v \times t. \quad (9)$$

Combining Eqs. (8) and (9) gives the following:

$$D = \left(\frac{6}{B \times \pi \times \sqrt{\pi}} \right)^{1/3} \times \sqrt{\frac{\eta}{v}} = C \times \sqrt{\frac{\Delta P}{v}}, \quad (10)$$

where in a first approximation, ignoring dynamic factors, we assume proportionality between flow rate and injection pressure ΔP via a constant C . Experimental results presented in Figs. 3(c) and 3(d) give $D \propto \Delta P^{0.36}/v^{0.44}$ in good agreement with this model.

While such an analysis roughly describes for the relationship of D and d with injection pressure ΔP and velocity v , there may be variations in the relationship, for various reasons as follows:

- (1) The fluid wets the substrate which changes the surface energy balance. We observed this when the substrate was changed.
- (2) The fluid injected by the micropipette requires a threshold value of ΔP , in function of its diameter.
- (3) The quantity of fluid injected by the micropipette is dependent on the particular geometry of its apex. Wall thickness seems to influence the droplet size, for instance.

Figure 2 show droplets of diameters ranging from 32 to 8.5 μm corresponding to volume ranging from 321 to 15 pl (assuming a spherical shape for the droplet). Further research should determine the three-dimensional shape of the droplets; for instance, some authors have proposed a hemisphere for microdroplets of 5 μm deposited on a glass coverslip.⁹ Note that generating droplets of hundreds of microns, in the nanoliter range, is easy with this setup. Conversely, in the example presented below droplets of 3 μm are generated, thus the femtoliter range is also attainable.

Finally, we illustrate the potential of our methodology in the field of particle generation, where small volume systems

offer promising properties.^{17,18} Figure 4(a) presents an array of monodisperse droplets of 3 μm containing NaCl 2.71M solution. Droplets slowly evaporate until supersaturation is established. A high supersaturation level is reached and a single nucleation event occurs, always yielding one single crystal of monodisperse size (740 \times 740 \times 370 nm³) per droplet [Fig. 4(b)], heights of crystals were measured by AFM. However, applications fields are not restricted to this field, as pointed out in the introduction.

In conclusion, we have developed a technique using a commercial microinjector coupled with an X, Y, and Z micromanipulator which is applicable to a range of materials and allows the production and storage of monodisperse microdroplets of aqueous phase in oil and without surfactant, maintaining control over size. Moreover, because isolated aqueous microdroplets are generated by micropipette, they can be manipulated individually by micropipette. Finally, this technology can be implemented in standard laboratory environments.

We thank ANR-06-Blan-0355 "MICROCRISTAL" and CEA Marcoule for financial supports. We thank A. Ranguis for AFM (CINaM), O. Grauby for SEM (CINaM), F. Bedu for spin coating (CINaM), T. Bactivelane (CINaM), B. Detailleur (CINaM), M. Audiffren (Anacrismat) for technical assistance, and to M. Sweetko for English revision.

¹A. Huebner, S. Sharma, M. Srisa-Art, F. Hollfelder, J. B. Edel, and A. J. deMello, *Lab Chip* **8**, 1244 (2008).

²O. A. Bempah and O. E. Hileman, Jr., *Can. J. Chem.* **51**, 3435 (1973).

³S. Y. Teh, R. Lin, L. H. Hung, and A. P. Lee, *Lab Chip* **8**, 198 (2008).

⁴S. L. Anna, N. Bontoux, and H. A. Stone, *Appl. Phys. Lett.* **82**, 364 (2003).

⁵R. Dreyfus, P. Tabeling, and H. Willaime, *Phys. Rev. Lett.* **90**, 144505 (2003).

⁶J. Liu, C. E. Nicholson, and S. J. Cooper, *Langmuir* **23**, 7286 (2007).

⁷B. Krämer, O. Hubner, H. Vortisch, L. Woste, T. Leisner, M. Schwell, E. Ruhl, and H. Baumgartel, *J. Chem. Phys.* **111**, 6521 (1999).

⁸K. Allain, R. Bebawee, and S. Lee, *Cryst. Growth Des.* **9**, 3183 (2009).

⁹K. T. Rodolfa, A. Bruckbauer, D. Zhou, A. I. Schevchuk, Y. E. Korchev, and D. Klenerman, *Nano Lett.* **6**, 252 (2006).

¹⁰S. A. Elrod, B. Hadimioglu, B. T. Khuri-Yakub, E. G. Rawson, E. Richley, C. F. Quate, N. N. Mansour, and T. S. Lundgren, *J. Appl. Phys.* **65**, 3441 (1989).

¹¹C.-Y. Lee, W. Pang, H. Yu, and E. S. Kim, *Appl. Phys. Lett.* **93**, 034104 (2008).

¹²H. Langer and H. Offermann, *J. Cryst. Growth* **60**, 389 (1982).

¹³F. Malloggi, N. Pannacci, R. Attia, F. Monti, P. Mary, H. Willaime, P. Tabeling, B. Cabane, and P. Poncet, *Langmuir* **26**, 2369 (2010).

¹⁴Saturated AgNO₃, KCl, KNO₃, CaSO₄·2H₂O, Na₂SO₄, glycine and sucrose solutions, and undersaturated proteins (bovine pancreatic trypsin inhibitor and lysozyme) in NaCl solutions.

¹⁵All the droplets are the same size because $2\sigma \approx 1$ pixel with the standard deviation $\sigma = 0.280 \mu\text{m}$ and 1 pixel = 0.5625 μm .

¹⁶A. S. Utada, E. Lorenceau, D. R. Link, P. D. Kaplan, H. A. Stone, and D. A. Weitz, *Science* **308**, 537 (2005).

¹⁷A. Y. Lee, I. S. Lee, S. S. Dette, J. Boerner, and A. S. Myerson, *J. Am. Chem. Soc.* **127**, 14982 (2005).

¹⁸R. Grossier and S. Veessler, *Cryst. Growth Des.* **9**, 1917 (2009).

AQ:
#3

AQ:
#5

AQ:
#6